

JOURNAL OF THE GEOTECHNICAL ENGINEERING DIVISION

SIMPLIFIED PROCEDURE FOR ESTIMATING DAM AND EMBANKMENT EARTHQUAKE-INDUCED DEFORMATIONS

By Faiz I. Makdisi,¹ A. M. ASCE and H. Bolton Seed,² F. ASCE

INTRODUCTION

In the past decade major advances have been achieved in analyzing the stability of dams and embankments during earthquake loading. Newmark (13) and Seed (18) proposed methods of analysis for predicting the permanent displacements of dams subjected to earthquake shaking and suggested this as a criterion of performance as opposed to the concept of a factor of safety based on limit equilibrium principles. Seed and Martin (26) used the shear beam analysis to study the dynamic response of embankments to seismic loads and presented a rational method for the calculation of dynamic seismic coefficients for earth dams. Ambraseys and Sarma (1) adopted the same procedure to study the response of embankments to a variety of earthquake motions.

Later the finite element method was introduced to study the two-dimensional response of embankments (5,7) and the equivalent linear method (21) was used successfully to represent the strain-dependent nonlinear behavior of soils. In addition the nature of the behavior of soils during cyclic loading has been the subject of extensive research (10,20,23,29). Both the improvement in the analytical tools to study the response of embankments and the knowledge of material behavior during cyclic loading led to the development of a more rational approach to the study of stability of embankments during seismic loading. Such an approach was used successfully to analyze the Sheffield Dam failure during the 1925 Santa Barbara earthquake (24) and the behavior of the San Fernando Dams during the 1971 earthquake (25). This method has since been used extensively in the design and analysis of many large dams in the State of California and elsewhere.

Note.—Discussion open until December 1, 1978. To extend the closing date one month, a written request must be filed with the Editor of Technical Publications, ASCE. This paper is part of the copyrighted Journal of the Geotechnical Engineering Division, Proceedings of the American Society of Civil Engineers, Vol. 104, No. GT7, July, 1978. Manuscript was submitted for review for possible publication on August 30, 1977.

¹Project Engr., Woodward-Clyde Consultants, San Francisco, Calif.

²Prof. of Civ. Engr., Univ. of California, Berkeley, Calif.

NUCLEAR REGULATORY COMMISSION

Docket No. 72-22 Official Ex. No. 102
In the matter of PFS
Staff _____ IDENTIFIED
Applicant _____ RECEIVED
Intervenor REJECTED _____
Cont'g. Off'r _____ DATE 6/20/02
Contractor _____ Witness Barklett
Other _____
Reporter C. Besa

DOCKETED
USNRC



2003 JAN 29 PM 3:09

OFFICE OF THE SECRETARY
RULEMAKINGS AND
ADJUDICATIONS STAFF

From the study of the performance of embankments during strong earthquakes, two distinct types of behavior may be discerned: (1) That associated with loose to medium dense sandy embankments, susceptible to rapid increases in pore pressure due to cyclic loading resulting in the development of pore pressures equal to the overburden pressure in large portions of the embankment, associated reductions in shear strength, and potentially large movements leading to almost complete failure; and (2) the behavior associated with compacted cohesive clays, dry sands, and some dense sands; here the potential for buildup of pore pressures is much less than that associated with loose to medium dense sands, the resulting cyclic strains are usually quite small, and the material retains most of its static undrained shearing resistance so that the resulting post-earthquake behavior is a limited permanent deformation of the embankment.

The dynamic analysis procedure proposed by Seed, et al. (25) has been used to predict adequately both types of embankment behavior using the "Strain Potential" concept. Procedures for integrating strain potentials to obtain the overall deformation of an embankment have been proposed by Seed, et al. (25), Lee (9), and Serff, et al. (27).

The dynamic analysis approach has been recommended by the Committee on Earthquakes of the International Commission on Large Dams (3): "high embankment dams whose failure may cause loss-of-life or major damage should be designed by the conventional method at first, followed by a dynamic analysis in order to investigate any deficiencies which may exist in the pseudo-static design of the dam." For low dams in remote areas the Committee recommended the use of conventional pseudostatic methods using a constant horizontal seismic coefficient selected on the basis of the seismicity of the area. However, the inadequacy of the pseudostatic approach to predict the behavior of embankments during earthquakes has been clearly recognized and demonstrated (19,24,25,26, 28). Furthermore in the same report (3) the Commission refers to the conventional method as follows: "There is a need for early revision of the conventional method since the results of dynamic analyses, model tests and observations of existing dams show that the horizontal acceleration due to earthquake forces varies throughout the height of the dam . . . in several instances, this method predicts a safe condition for dams which are known to have had major slides."

It is this need for a simple yet rational approach to the seismic design of small embankments that prompted the development of the simplified procedure described herein.

This approximate method uses the concept originally proposed by Newmark (13) for calculating permanent deformations but it is based on an evaluation of the dynamic response of the embankment as proposed by Seed and Martin (26) rather than rigid body behavior. It assumes that failure occurs on a well-defined slip surface and that the material behaves elastically at stress levels below failure but develops a perfectly plastic behavior above yield. The method involves the following steps:

1. A yield acceleration, i.e., an acceleration at which a potential sliding surface would develop a factor of safety of unity is determined. Values of yield acceleration are a function of the embankment geometry, the undrained strength of the material (or the reduced strength due to shaking), and the location of the potential sliding mass.

2. Earthquake induced accelerations in the embankment are determined using dynamic response analyses. Finite element procedures using strain-dependent soil properties can be used for calculating time histories of acceleration, or simpler one-dimensional techniques might be used for the same purpose. From these analyses, time histories of average accelerations for various potential sliding masses can be determined.

3. For a given potential sliding mass, when the induced acceleration exceeds the calculated yield acceleration, movements are assumed to occur along the direction of the failure plane and the magnitude of the displacement is evaluated by a simple double integration procedure.

The method has been applied to dams with heights in the range of 100 ft-200 ft (30 m-60 m), and constructed of compacted cohesive soils or very dense cohesionless soils, but may be applicable to higher embankments. A similar approach has been proposed by Sarma (16) using the assumption of a rigid block on an inclined plane rather than a deformable earth structure that responds with differential motions to the imposed base excitation.

In the following sections the steps involved in the analyses will be described in detail and design curves prepared on the basis of analyzed cases will be presented, together with an example problem to illustrate the use of the method. Note, however, that the method is an approximate one and involves simplifying assumptions. The design curves are averages based on a limited number of cases analyzed and should be updated as more data become available and more cases are studied.

DETERMINATION OF YIELD ACCELERATION

The yield acceleration, k_y , is defined as that average acceleration producing a horizontal inertia force on a potential sliding mass so as to produce a factor of safety of unity and thus cause it to experience permanent displacements.

For soils that do not develop large cyclic strains or pore pressures and maintain most of their original strength after earthquake shaking, the value of k_y can be calculated by stability analyses using limiting equilibrium methods. In conventional slope stability analyses the strength of the material is defined as either the maximum deviator stress in an undrained test, or the stress level that would cause a certain allowable axial strain, say 10%, in a test specimen. However, the behavior of the material under cyclic loading conditions is different than that under static conditions. Due to the transient nature of the earthquake loading, an embankment may be subjected to a number of stress pulses at levels equal to or higher than its static failure stress that simply produce some permanent deformation rather than complete failure. Thus the yield strength is defined, for the purpose of this analysis, as that maximum stress level below which the material exhibits a near elastic behavior (when subjected to cyclic stresses of numbers and frequencies similar to those induced by earthquake shaking) and above which the material exhibits permanent plastic deformation of magnitudes dependent on the number and frequency of the pulses applied. Fig. 1 shows the concept of cyclic yield strength. The material in this case has a cyclic yield strength equal to about 90% of its static undrained strength and as shown in Fig. 1(a) the application of 100 cycles of stress amounting to 80%

of the undrained strength resulted in essentially an elastic behavior with very little permanent deformation. On the other hand, the application of 10 cycles of stress level equal to 95% of the static undrained strength led to substantial permanent strain as shown in Fig. 1(b). On loading the material monotonically to failure after the series of cyclic stress applications, the material was found to retain the original undrained strength. This type of behavior is associated with various types of soils that exhibit small increases in pore pressure during cyclic loading. This would include clayey materials, dry or partially saturated cohesionless soils, or very dense saturated cohesionless materials that will not undergo significant deformations, even under cyclic loading conditions, unless the undrained static strength of the soil is exceeded.

Seed and Chan (20) conducted cyclic tests on samples of undisturbed and compacted silty clays and found that for conditions of no stress reversal and for different values of initial and cyclic stresses, the total stress required to produce large deformations in 10 cycles and 100 cycles ranged between 90%–110% of the undrained static strength.

Sangroy, et al. (15) investigated the effective stress response of clay under repeated loading. They tested undisturbed samples of clay (LL = 28, PI = 10) and found that the cyclic yield strength of this material was of the order of 60% of its static undrained strength.

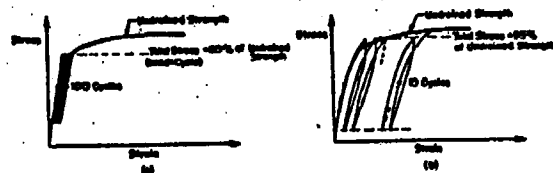


FIG. 1.—Determination of Dynamic Yield Strength

Rahman (14) performed similar tests on remolded samples of a brittle silty clay (LL = 91, PI = 49) and found that the cyclic yield strength was a function of the initial effective confining pressure. For practical ranges of effective confining pressures the cyclic yield strength for this material ranged between 80%–95% of its static undrained strength. At cyclic stress levels below the yield strength, in all cases, the material reached equilibrium and assumed an elastic behavior at strain levels less than 2% irrespective of the number of stress cycles applied.

Thiers and Seed (28) performed tests on undisturbed and remolded samples of different clayey materials to determine the reduction in static undrained strength due to cyclic loading. Their results are summarized in Fig. 2 which shows the reduction in undrained strength after cyclic loading as a function of the ratio of the "maximum cyclic strain" to the "static failure strain." These results were obtained from strain controlled cyclic tests; after the application of 200 cycles of a certain strain amplitude, the sample was loaded to failure monotonically at a strain rate of 3%/min. Thus from Fig. 2 it could be argued that if a clay is subjected to 200 cycles of strain with an amplitude less than half its static failure strain, the material may be expected to retain at least 90% of its original static undrained strength.

Andersen (2), on the basis of cyclic simple shear tests on samples of Drammen clay, determined that the reduction in undrained shear strength was found to be less than 25% as long as the cyclic shear strain was less than $\pm 3\%$ even after 1,000 cycles. Some North Sea clays, however, have shown a strength reduction of up to 40% for the same level of cyclic loading.

On the basis of the experimental data reported previously and for values

TABLE 1.—Maximum Cyclic Shear Strains Calculated from Dynamic Finite Element Response Analyses

Magnitude (1)	Embankment height, in feet (2)	Slope, H:V (3)	Maximum base acceleration, g (4)	Maximum shear strain, as a percentage (5)
6-1/2 (Caltech record)	75	2:1	0.5	0.2–0.4
6-1/2 (Caltech record)	150	2:1	0.2	0.1–0.15
6-1/2 (Caltech record)	150	2:1	0.5	0.2–0.3
6-1/2 (Lake Hughes record)	150	2:1	0.2	0.1–0.15
6-1/2 (Caltech record)	150	2-1/2:1	0.5	0.2–0.3
7-1/2 (Taft record)	150	2:1	0.5	0.2–0.5
7-1/2 (Taft record)	150	2:1	0.2	0.1–0.2
8-1/4 (S-I record)	150	2:1	0.75	0.4–1.0
8-1/4 (S-I record)	135	—	0.4	0.2–0.5

Note: 1 ft = 0.305 m.

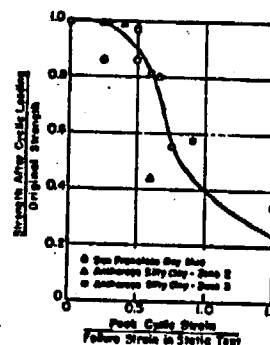


FIG. 2.—Reduction in Static Undrained Strength Due to Cyclic Loading (29)

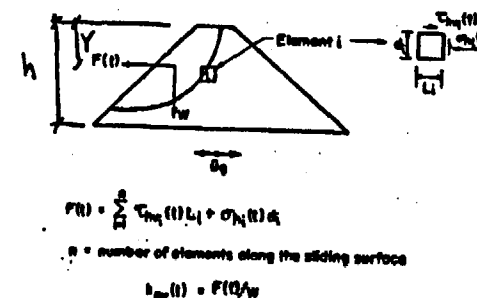


FIG. 3.—Calculation of Average Acceleration from Finite Element Response Analysis

of cyclic shear strains calculated from earthquake response analyses, the value of cyclic yield strength for a clayey material can be estimated. In most cases this value would appear to be 80% or more of the static undrained strength. This value in turn may be used in an appropriate method of stability analysis to calculate the corresponding yield acceleration.

Finite element response analyses (as will be described later) have been carried out to calculate time histories of crest acceleration and average acceleration

for various potential sliding masses. The method of analysis employs the equivalent linear technique with strain-dependent modulus and damping. The ranges of calculated maximum shear strains, for different magnitude earthquakes and different embankment characteristics, are presented in Table 1. It can be seen from Table 1 that the maximum cyclic shear strain induced during the earthquakes ranged between 0.1% for a magnitude 6-1/2 earthquake with a base acceleration of 0.2 g and 1% for a magnitude 8-1/4 earthquake with a base acceleration of 0.75 g. For the compacted clayey material encountered in dam embankments "static failure strain" values usually range between 3%-10%, depending on whether the material was compacted on the dry or wet side of the optimum moisture content. Thus in both instances the ratio of the "cyclic strain" to "static failure strain" is less than 0.5. $\Rightarrow 90\%$ STRENGTH

It seems reasonable, therefore, to assume that for these compacted cohesive soils, very little reduction in strength may be expected as a result of strong earthquake loading of the magnitude described previously.

Once the cyclic yield strength is defined, the calculation of the yield acceleration can be achieved by using one of the available methods of stability analysis. In the present study the ordinary method of slices has been used to calculate the yield acceleration for circular slip surfaces using a pseudostatic analysis. As an alternative one of the writers (18) has suggested a method of combining both effective and total stress approaches, where the shear strength on the failure plane during the earthquake is considered to be a function of the initial effective normal stress on that same plane before the earthquake. This method is applicable to noncircular slip surfaces and the horizontal inertia force resulting in a factor of safety of unity can readily be calculated.

Having determined the yield acceleration for a certain location of the slip surface, the next step in the analysis is to determine the time history of earthquake-induced average accelerations for that particular sliding mass. This will be treated in the following section.

DETERMINATION OF EARTHQUAKE INDUCED ACCELERATION

In order for the permanent deformations to be calculated for a particular slip surface, the time history of earthquake induced average accelerations must first be determined.

Two-dimensional finite element procedures using equivalent linear strain-dependent properties are available (6) and have been shown to provide response values in good agreement with measured values (8) and with closed-form one-dimensional wave propagation solutions (17).

For most of the case studies of embankments used in the present analysis, the response calculation was performed using the finite element computer program QUAD-4 (6) with strain-dependent modulus and damping. The program uses the Rayleigh damping approach and allows for variable damping to be used in different elements.

To calculate the time history of average acceleration for a specified sliding mass, the method described by Chopra (4) was adopted in the present study. The finite element calculation provides time histories of stresses for every element in the embankment. As shown in Fig. 3, at each time step the forces acting along the boundary of the sliding mass are calculated from the corresponding

normal and shear stresses of the finite elements along that boundary. The resultant of these forces divided by the weight of the sliding mass would give the average acceleration, $k_{av}(t)$, acting on the sliding mass at that instant in time. The process is repeated for every time step to calculate the entire time history of average acceleration.

For a 150-ft (46-m) high dam subjected to 30 sec of the Taft earthquake record scaled to produce a maximum base acceleration of 0.2 g, the variation

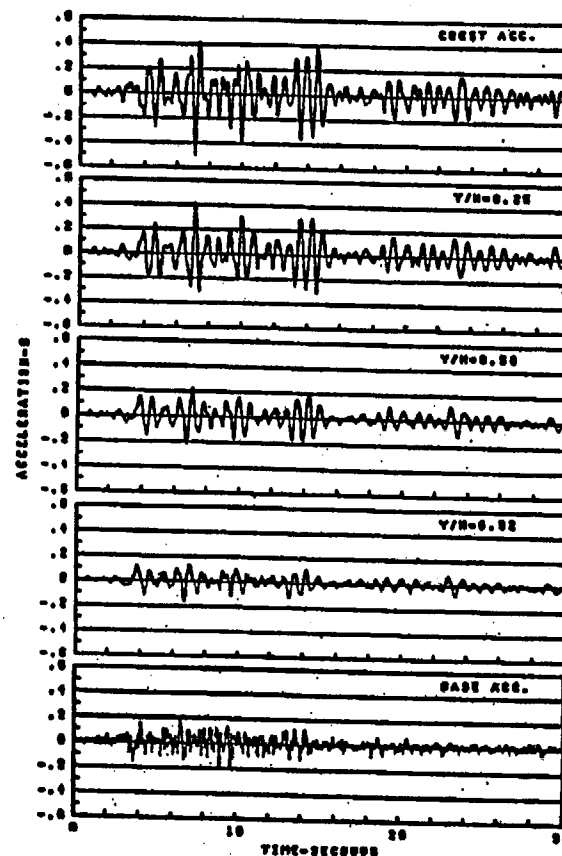


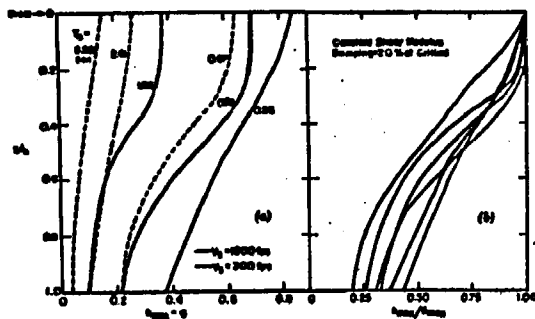
FIG. 4.—Time Histories of Average Acceleration for Various Depths of Potential Sliding Mass

of the time history of k_{av} with the depth of the sliding mass within the embankment, together with the time history of crest accelerations, is shown in Fig. 4.

Comparing the time history of crest acceleration with that of the average acceleration for different depths of the potential sliding mass, the similarity in the frequency content is readily apparent (it generally reflects the first natural period of the embankment), while the amplitudes are shown to decrease as the depth of the sliding mass increases towards the base of the embankment. The maximum crest acceleration is designated by \ddot{u}_{max} , and k_{max} is the maximum

average acceleration for a potential sliding mass extending to a specified depth, y .

It would be desirable to establish a relationship showing the variation of the maximum acceleration ratio, k_{max}/\ddot{u}_{max} , with depth for a range of embankments and earthquake loading conditions. It would then be sufficient, for design purposes, to estimate the maximum crest acceleration in a given embankment due to a specified earthquake and use this relationship to determine the maximum average acceleration for any depth of the potential sliding mass. A simplified procedure to estimate the maximum crest acceleration and the natural period



CALCULATION OF PERMANENT DEFORMATIONS

Once the yield acceleration and the time history of average induced acceleration for a potential sliding mass have been determined, the permanent displacements can readily be calculated.

By assuming a direction of the sliding plane and writing the equation of

TABLE 2.—Embankment Characteristics for Magnitude 6-1/2 Earthquake

Case number (1)	Embankment description (2)	Height, in feet (3)	Base acceleration, g (4)	T_0 , in seconds (5) ^a	k_{max} , g (6) ^b	Symbol ^c (7)
1	Example slope = 2:1 $k_{2max} = 60$	150	0.2 (Caltech record)	0.8	(1) 0.31 (2) 0.12	● ■
2	Example slope = 2:1 $k_{2max} = 60$	150	0.5 (Caltech record)	1.08	(1) 0.4 (2) 0.18	○ □
3	Example slope = 2:1 $k_{2max} = 80$	150	0.5 (Lake Hughes record)	0.84	(1) 0.33 (2) 0.16	⊙ △
4	Example slope = 2-1/2:1 $k_{2max} = 80$	150	0.5 (Caltech record)	0.95	(1) 0.49 (2) 0.22	◇ ▽
5	Example slope = 2:1 $k_{2max} = 60$	75	0.5 (Caltech record)	0.6	(1) 0.86 (2) 0.26	⊙ ■

^a Calculated first natural period of the embankment.

^b Maximum value of time history of: (1) Crest acceleration; and (2) average acceleration for sliding mass extending through full height of embankment.

^c Legend used in Fig. 9(a).

Note: 1 ft = 0.305 m.

motion for the sliding mass along such a plane, the displacements that would occur any time the induced acceleration exceeds the yield acceleration may be evaluated by simple numerical integration. For the purposes of the soil types considered in this study, the yield acceleration was assumed to be constant throughout the earthquake.

The direction of motion for a potential sliding mass once yielding occurs

was assumed to be along a horizontal plane. This mode of deformation is not uncommon for embankments subjected to strong earthquake shaking, and is manifested in many cases in the field by the development of longitudinal cracks along the crest of the embankment. However studies made for other directions of the sliding surface showed that this factor had little effect on the computed displacements (11).

To calculate an order of magnitude of the deformations induced in embankments due to strong shaking a number of cases have been analyzed during the course of this study. The height of embankments considered ranged between 75 ft–150 ft (23 m–46 m) with varying slopes and material properties. The embankments were subjected to ground accelerations representing three different earthquake magnitudes: 6-1/2, 7-1/2, and 8-1/4.

The method used for calculating the response, as mentioned earlier, is a time-step finite element analysis using the equivalent linear method. The strain-dependent modulus and damping relations for the soils used in this study are

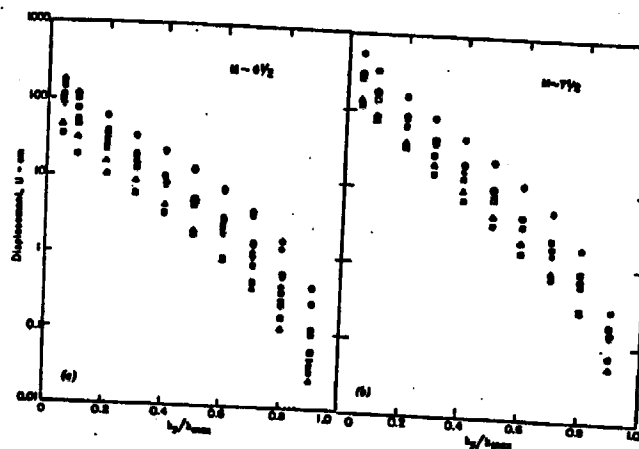


FIG. 9.—Variation of Permanent Displacement with Yield Acceleration: (a) Magnitude 6-1/2 Earthquake; (b) Magnitude 7-1/2 Earthquake

presented in Fig. 8. The response computation for each base motion was repeated for a number of iterations (mostly 3–4) until strain compatible material properties were obtained. In each case both time histories of crest acceleration and the average acceleration for a potential sliding mass extending through almost the full height of the embankment were calculated, together with the first natural period of the embankment. In one case however, time histories of average acceleration for sliding surfaces at five different levels in the embankment were obtained (see Fig. 4), and the corresponding permanent deformations for each time history were calculated for different values of yield acceleration. It was found that for the same ratio of yield acceleration to maximum average acceleration at each level, the computed deformations varied uniformly between a maximum value obtained using the crest acceleration time history to a minimum value obtained using the time history of average acceleration for a sliding mass extending through the full height of the embankment. Thus it was concluded

sufficient for the remaining cases to compute the deformations only for these two levels.

Table 2 shows details of the embankments analyzed using ground motions representative of a magnitude 6-1/2 earthquake. The two rock motions used were those recorded at the Cal Tech Seismographic Laboratory (S90W Component) and at Lake Hughes Station No. 12 (N12E) during the 1971 San Fernando earthquake, with maximum accelerations scaled to 0.2 g and 0.5 g. The computed natural periods and maximum values of the acceleration time histories are also presented in Table 2. The computed natural periods ranged between a value of 0.6 sec for the 75-ft (23-m) high embankment to a value of 1.08 sec for the 150-ft (46-m) high embankment. Because of the nonlinear strain-dependent

TABLE 3.—Embankment Characteristics for Magnitude 7-1/2 Earthquake

Case number (1)	Embankment description (2)	Height, in feet (3)	Base acceleration, g (4)	T_n , in seconds (5) ^a	k_{max} , g (8) ^b	Symbol ^c (7)
1	Example slope = 2:1 $k_{2max} = 60$	150	0.2 (Taft record)	0.86	(1) 0.41	●
					(2) 0.13	■
2	Example slope = 2:1 $k_{2max} = 60$	150	0.5 (Taft record)	1.18	(1) 0.54	○
					(2) 0.21	□
3	Example slope = 2-1/2:1 $k_{2max} = 80$	150	0.2 (Taft record)	0.76	(1) 0.46	⊙
					(2) 0.15	△

^aCalculated first natural period of the embankment.

^bMaximum value of time history of: (1) Crest acceleration; and (2) average acceleration for sliding mass extending through full height of embankment.

^cLegend used in Fig. 9(b).

Note: 1 ft = 0.305 m.

behavior of the material, the response of the embankment is highly dependent on the amplitude of the base motion. This is clearly demonstrated in the first two cases in Table 2, where the same embankment was subjected to the same ground acceleration history but with different maximum accelerations for each case. In one instance, for a base acceleration of 0.2 g the calculated maximum crest accelerations was 0.3 g with a magnification of 1.5 and a computed natural period of the order of 0.8 sec. In the second case, for a base acceleration of 0.5 g the computed maximum crest acceleration was 0.4 g with an attenuation of 0.8 and a computed natural period of 1.1 sec.

From the time histories of induced acceleration calculated for all the cases

described in Table 2 and for various ratios of yield acceleration to maximum average acceleration, k_y/k_{max} , the permanent deformations were calculated by numerical double integration. The results are presented in Fig. 9(a) which shows that for relatively low values of yield acceleration, k_y/k_{max} of 0.2 for example, the range of computed permanent displacements was of the order of 10 cm-70 cm (4 in.-28 in.). However, for larger values of k_y/k_{max} , say 0.5 or more, the calculated displacements were less than 12 cm (4.8 in.). It should be emphasized that for very low values of yield accelerations (in this case $k_y/k_{max} \leq 0.1$) the basic assumptions used in calculating the response by the finite element

TABLE 4.—Embankment Characteristics of Magnitude 8-1/4 Earthquake

Case number (1)	Embankment description (2)	Height, in feet (3)	Base acceleration, g (4)	T_n , in seconds (5) ^a	k_{max} , g (8) ^b	Symbol ^c (7)
1	Chabot Dam (average properties)	135	0.4 (S-I Synth. record)	0.99	(1) 0.57	○
	Chabot Dam (Lower bound)	135	0.4 (S-I Synth. record)	1.07	(1) 0.53	△
	Chabot Dam (Upper bound)	135	0.4	0.83	(1) 0.68	□
2	Example slope = 2:1 $k_{2max} = 60$	150	0.75	1.49	(1) 0.74 (2) 0.34	● ■

^aCalculated first natural period of the embankment.

^bMaximum value of time history of: (1) Crest acceleration; and (2) average acceleration for sliding mass extending through full height of embankment.

^cLegend used in Fig. 10(a).

Note: 1 ft = 0.305 m.

method, i.e., the equivalent linear behavior and the small strain theory, become invalid. Consequently, the acceleration time histories calculated for such a case do not represent the real field behavior and the calculated displacements based on these time histories may not be realistic.

The procedure described previously was repeated for the case of a magnitude 7-1/2 earthquake. The base acceleration time history used for this analysis was that recorded at Taft during the 1952 Kern County earthquake and scaled to maximum accelerations of 0.2 g and 0.5 g. The details of the three cases analyzed are presented in Table 3 and the results of the computations of the

permanent displacements are shown in Fig. 9(b). For a ratio of k_y/k_{max} of 0.2 the calculated displacements in this case ranged between 30 cm–200 cm (12 in.–80 in.), and for ratios greater than 0.5 the displacements were less than 25 cm (0.8 ft).

In the cases analyzed for the 8-1/4 magnitude earthquake, an artificial accelerogram proposed by Seed and Idriss (21) was used with maximum base accelerations of 0.4 g and 0.75 g. Two embankments were analyzed in this case and their calculated natural periods ranged between 0.8 sec and 1.5 sec. Table 4 shows the details of the calculations and in Fig. 10(a) the results of the permanent displacement computations are presented. As can be seen from Fig. 10(a) the permanent displacements computed for a ratio of k_y/k_{max} of 0.2 ranged between 200 cm–700 cm (80 in.–28 in.), and for ratios higher than 0.5 the values were less than 100 cm (40 in.). Note in this case that values of deformations calculated for a yield ratio less than 0.2 may not be realistic.

An envelope of the results obtained for each of the three earthquake loading

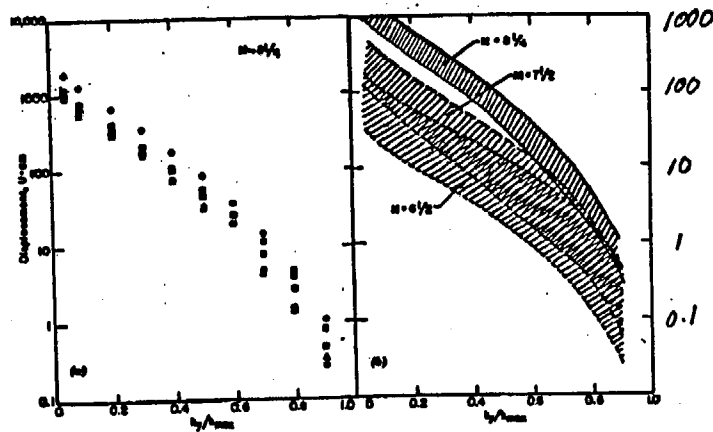


FIG. 10.—Variation of Permanent Displacement with Yield Acceleration: (a) Magnitude 8-1/4 Earthquake; (b) Summary of All Data

conditions is presented in Fig. 10(b) and reveals a large scatter in the computed results reaching, in the case of the magnitude 6-1/2 earthquake, about one order of magnitude.

It can reasonably be expected that for a potential sliding mass with a specified yield acceleration, the magnitude of the permanent deformation induced by a certain earthquake loading is controlled by the following factors: (1) The amplitude of induced average accelerations, which is a function of the base motion, the amplifying characteristics of the embankment, and the location of the sliding mass within the embankment; (2) the frequency content of the average acceleration time history, which is governed by the embankment height and stiffness characteristics, and is usually dominated by the first natural frequency of the embankment; and (3) the duration of significant shaking, which is a function of the magnitude of the specified earthquake.

Thus to reduce the large scatter exhibited in the data in Fig. 10(b), the permanent

displacements for each embankment were normalized with respect to its calculated first natural period, T_n , and with respect to the maximum value, k_{max} , of the average acceleration time history used in the computation. The resulting normalized permanent displacements for the three different earthquakes are presented in Fig. 11(a). It may be seen that a substantial reduction in the scatter of the data is achieved by this normalization procedure as evidenced by comparing the results in Figs. 10(b) and 11(a). This shows that for the ranges of embankment heights considered in this study [75 ft–150 ft (50 m–65 m)] the first natural period of the embankment and the maximum value of acceleration time history may be considered as two of the parameters having a major influence on the calculated permanent displacements. Average curves for the normalized permanent displacements based on the results in Fig. 11(a) are presented in Fig. 11(b). Although some scatter still exists in the results as shown in Fig. 11(a), the average curves presented in Fig. 11(b) are considered adequate to provide an order of magnitude of the induced permanent displacements for different

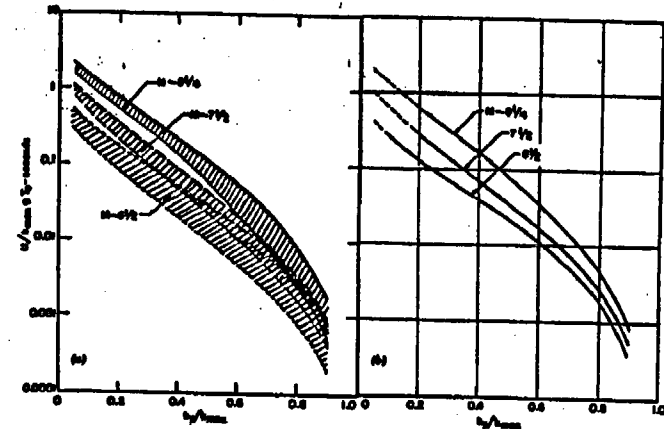


FIG. 11.—Variation of Yield Acceleration with: (a) Normalized Permanent Displacement—Summary of All Data; and (b) Average Normalized Displacement.

magnitude earthquakes. At yield acceleration ratios less than 0.2 the average curves are shown as dashed lines since, as mentioned earlier, the calculated displacements at these low ratios may be unrealistic.

Thus, to calculate the permanent deformation in an embankment constructed of a soil that does not change in strength significantly during an earthquake, it is sufficient to determine its maximum crest acceleration, \ddot{u}_{max} , and first natural period, T_n , due to a specified earthquake. Then by the use of the relationships presented in Fig. 7, the maximum value of average acceleration history, k_{max} , for any level of the specified sliding mass may be determined. Entering the curves in Fig. 11(b) with the appropriate values of k_{max} and T_n , the permanent displacements can be determined for any value of yield acceleration associated with that particular sliding surface.

It has been assumed earlier in this paper that in the majority of embankments, permanent deformations usually occur due to slip of a sliding mass on a horizontal failure plane. For those few instances where sliding might occur on an inclined

PLUS A PSEUDOSTATIC ANALYSIS TO GET k_y

failure plane it is of interest to determine the difference between the actual deformations and those calculated with the assumption of a horizontal failure plane having the same yield acceleration. A simple computation was made to investigate this condition using the analogy of a block on an inclined plane for a purely frictional material. It was found that for inclined failure planes with slope angles of 15° to the horizontal, the computed displacements were 10%–18% higher than those based on a horizontal plane assumption.

APPLICATION OF METHOD TO EMBANKMENT SUBJECTED TO 8-1/4 MAGNITUDE EARTHQUAKE

To illustrate the use of the simplified procedure for evaluating earthquake-induced deformations, computations are presented herein for the 135-ft (41-m) high Chabot Dam, constructed of sandy clay and having the section shown in Fig. 12.

The shear wave velocity of the embankment was determined from a field investigation and the strain-dependent modulus and damping were determined from laboratory tests on undisturbed samples. The dam, located about 20 miles

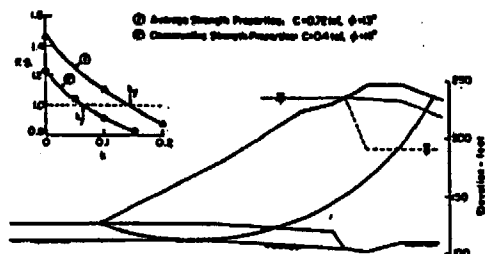


FIG. 12.—Yield Acceleration Values for Slide Mass Extending through Full Height of Embankment

(32 km) from the San Andreas fault, was shaken in 1906 by the magnitude 8-1/4 San Francisco earthquake with no significant deformations being noted; peak accelerations in the rock underlying the dam in this event are estimated to have been about 0.4 g. Accordingly the response of the embankment to ground accelerations representative of a magnitude 8-1/4 earthquake and having a maximum acceleration of 0.4 g was calculated by a finite element analysis. The maximum crest acceleration of the embankment, \ddot{u}_{max} , was calculated to be 0.57 g and the first natural period, $T_0 = 0.99$ sec. The maximum values of the calculated shear strain were less than 0.5%. On the basis of static undrained tests on the embankment material, the static failure strains ranged between 3%–8%, so that for the purposes of this analysis the cyclic yield strength of this material can be considered equal to its static undrained strength. From consolidated undrained tests on representative samples of the embankment material two interpretations were made for the strength of the material: (1) Based on an average of all the samples tested resulting in a cohesion value, c , of 0.72 tsf (69 kN/m²) and a friction angle, ϕ , of 13°; and (2) a conservative interpretation, based on the minimum strength values with a cohesion of 0.4

tsf (38 kN/m²) and a friction angle of 16°. Using these strength estimates, values of yield accelerations were calculated for a sliding mass extending through the full height of the embankment as shown in Fig. 12.

Considering the average relationship of k_{max}/\ddot{u}_{max} with depth shown in Fig. 7, the ratio for a sliding mass extending through the full height of the embankment ($y/h = 0.95$) is 0.35, resulting in a maximum average acceleration, k_{max} , of $0.35 \times 0.57 g = 0.2 g$. From Fig. 12 the yield acceleration calculated for the average strength values is 0.14 g. Thus the parameters to be used in Fig. 11(b) to calculate the displacements for this particular sliding surface are as follows: magnitude = 8-1/4; $T_0 = 0.99$ sec; $k_{max} = 0.2$; and $k_y/k_{max} = 0.14/0.20 = 0.7$. From Fig. 11(b): $U/k_{max} T_0 = 0.013$ sec, therefore, the displacement $U = 0.013 \times 0.2 \times 32.2 \times 0.99 = 0.08$ ft (0.02 m).

Using the most conservative value of k_{max}/\ddot{u}_{max} shown in Fig. 7 of 0.47, the computed displacement would have been 0.58 ft (0.18 m). Similarly using the conservative strength parameters for the soil (giving $k_y = 0.07$) and the average curve for k_{max}/\ddot{u}_{max} shown in Fig. 7, the computed displacement would have been 1.5 ft (0.45 m). All of these values are in reasonable accord with the observed performance of the dam during the 1906 earthquake.

The calculation was repeated for a sliding mass extending through half the depth of the embankment. The computed permanent displacements ranged between 0.02 ft–1.08 ft (0.006 m–0.33 m) indicating that the critical potential sliding mass in this case was that extending through the full height of the embankment.

CONCLUSIONS

A simple yet rational approach to the design of small embankments under earthquake loading has been described herein. The method is based on the concept of permanent deformations as proposed by Newmark (13) but modified to allow for the dynamic response of the embankment as proposed by Seed and Martin (26) and restricted in application to compacted clayey embankments and dry or dense cohesionless soils that experience very little reduction in strength due to cyclic loading. The method is an approximate one and involves a number of simplifying assumptions that may lead to somewhat conservative results.

On the basis of response computations for embankments subjected to different ground motion records, a relationship for the variation of induced average acceleration with embankment depth has been established. Design curves to estimate the permanent deformations for embankments, in the height range of 100 ft–200 ft (30 m–60 m), have been established based on equivalent linear finite element dynamic analyses for different magnitude earthquakes. The use of these curves requires a knowledge of the maximum crest acceleration and the natural period of an embankment due to a specified ground motion.

It should be noted that the design curves presented are based on averages of a range of results that exhibit some degree of scatter, and are derived from a limited number of cases. These curves should be updated and refined as analytical results for more embankments are obtained.

Finally, the method has been applied to an actual embankment that was subjected to a magnitude 8-1/4 earthquake at an epicentral distance of some 20 miles. Depending on the degree of conservatism in estimating the undrained

strength of the material and in estimating the maximum accelerations in the embankment, the calculated deformations for this 135-ft (40-m) clayey embankment ranged between 0.1 ft-1.5 ft (0.3 m-0.46 m). These approximate displacement values are in good accord with the actual performance of the embankment during the earthquake.

Whereas the method described herein provides a rational approach to the design of embankments and offers a significant improvement over the conventional pseudostatic approach, the nature of the approximations involved requires that it be used with caution and good judgment especially in determining the soil characteristics of the embankment to which it may be applied.

For large embankments, for embankments where failure might result in a loss of life or major damage and property loss, or where soil conditions cannot be determined with a significant degree of accuracy to warrant the use of the method, the more rigorous dynamic method of analysis described earlier might well provide a more satisfactory alternative for design purposes.

Acknowledgment

The study described in this paper was conducted under the sponsorship of the National Science Foundation (Grant ENV 75-21875). The support of the National Science Foundation is gratefully acknowledged.

Appendix.—References

1. Ambrascy, N. N., and Sarma, S. K., "The Response of Earth Dams to Strong Earthquakes," *Geotechnique*, London, England, Vol. 17, Sept., 1967, pp. 181-213.
2. Andersen, K. H., "Behavior of Clay Subjected to Undrained Cyclic Loading," *Proceedings, Conference on Behavior of Off-Shore Structures*, Trondheim, Norway, Vol. 1, 1976, pp. 392-403.
3. "A Review of Earthquake Resistant Design of Dams," *Bulletin 27*, International Commission on Large Dams, Mar., 1975.
4. Chopra, A. K., "Earthquake Effects on Dams," thesis presented to the University of California, at Berkeley, Calif., in 1966, in partial fulfillment of the requirements for the degree of Doctor of Philosophy.
5. Clough, R. W., and Chopra, A. K., "Earthquake Stress Analysis in Earth Dams," *Journal of the Engineering Mechanics Division*, ASCE, Vol. 92, No. EM2, Proc. Paper 4793, Apr., 1966, pp. 197-212.
6. Idriss, I. M., et al., "QUAD-4, A Computer Program for Evaluating the Seismic Response of Soil Structures by Variable Damping Finite Elements," *Report No. EERC 73 16*, Earthquake Engineering Research Center, University of California, Berkeley, Calif., June, 1973.
7. Idriss, I. M., and Seed, H. B., "Response of Earth Banks During Earthquakes," *Journal of the Soil Mechanics and Foundations Division*, ASCE, Vol. 93, No. SM3, Proc. Paper 5232, May, 1967, pp. 61-82.
8. Kovacs, W. D., Seed, H. B., and Idriss, I. M., "Studies of Seismic Response of Clay Banks," *Journal of the Soil Mechanics and Foundations Division*, ASCE, Vol. 97, No. SM2, Proc. Paper 7878, Feb., 1971, pp. 441-455.
9. Lee, K. L., "Seismic Permanent Deformations in Earth Dams," *Report No. UCLA-ENG-7497*, School of Engineering and Applied Science, University of California at Los Angeles, Los Angeles, Calif., Dec., 1974.
10. Lee, K. L., and Seed, H. B., "Dynamic Strength of Anisotropically Consolidated Sand," *Journal of the Soil Mechanics and Foundations Division*, ASCE, Vol. 93, No. SM3, Proc. Paper 5451, Sept., 1967, pp. 169-190.
11. Makdisi, F. I., and Seed, H. B., "A Simplified Procedure for Computing Maximum

12. Martin, G. R., "The Response of Earth Dams to Earthquakes," thesis presented to the University of California, at Berkeley, Calif., in 1963, in partial fulfillment of the requirements for the degree of Doctor of Philosophy.
13. Newmark, N. M., "Effects of Earthquakes on Dams and Embankments," *Geotechnique*, London, England, Vol. 5, No. 2, June, 1965.
14. Rahman, M. S., "Undrained Behavior of Saturated Normally Consolidated Clay Under Repeated Loading," thesis presented to the Indian Institute of Technology, at Kharagpur, India, in July, 1972, in partial fulfillment of the requirements for the degree of Master of Science.
15. Sangrey, D., Hentel, D., and Ertig, M., "The Effective Stress Response of a Saturated Clay Soil to Repeated Loading," *Canadian Geotechnical Journal*, Vol. 6, No. 3, Aug., 1969, pp. 241-252.
16. Sarma, S. K., "Seismic Stability of Earth Dams and Embankments," *Geotechnique*, London, England, Vol. 25, No. 4, Dec., 1975, pp. 743-761.
17. Schnabel, P. B., and Seed, H. B., "Accelerations in Rock for Earthquakes in the Western United States," *Report No. EERC 72-2*, Earthquake Engineering Research Center, University of California, Berkeley, Calif., July, 1972.
18. Seed, H. B., "A Method for Earthquake-Resistant Design of Earth Dams," *Journal of the Soil Mechanics and Foundations Division*, ASCE, Vol. 92, No. SM1, Proc. Paper 4616, Jan., 1966, pp. 13-41.
19. Seed, H. B., "A Case Study of Seismic Instability and Terzaghi Foresight," Terzaghi Memorial Lecture Program, Bogazici University, Istanbul, Turkey, Aug. 14-16, 1975.
20. Seed, H. B., and Chan, C. K., "Clay Strength Under Earthquake Loading Conditions," *Journal of the Soil Mechanics and Foundations Division*, ASCE, Vol. 92, No. SM2, Proc. Paper 4723, Mar., 1966, pp. 53-78.
21. Seed, H. B., and Idriss, I. M., "Rock Motion Accelerograms for High Magnitude Earthquakes," *Report No. EERC 67-7*, Earthquake Engineering Research Center, University of California, Berkeley, Calif., Apr., 1969.
22. Seed, H. B., and Idriss, I. M., "Influence of Soil Conditions on Ground Motions During Earthquakes," *Journal of the Soil Mechanics and Foundations Division*, ASCE, Vol. 95, No. SM1, Proc. Paper 6347, Jan., 1969, pp. 99-137.
23. Seed, H. B., and Lee, K. L., "Liquefaction of Saturated Sands During Cyclic Loading," *Journal of the Soil Mechanics and Foundations Division*, ASCE, Vol. 92, No. SM6, Proc. Paper 4972, Nov., 1966, pp. 105-134.
24. Seed, H. B., Lee, K. L., and Idriss, I. M., "Analysis of the Sheffield Dam Failure," *Journal of the Soil Mechanics and Foundations Division*, ASCE, Vol. 95, No. SM6, Proc. Paper 6906, Nov., 1969, pp. 1453-1490.
25. Seed, H. B., et al., "Analysis of the Slides in the San Fernando Dams during the Earthquake of February 9, 1971," *Report No. EERC 73-2*, Earthquake Engineering Research Center, University of California, Berkeley, Calif., June, 1973.
26. Seed, H. B., and Martin, G. R., "The Seismic Coefficient in Earth Dam Design," *Journal of the Soil Mechanics and Foundations Division*, ASCE, Vol. 92, No. SM3, Proc. Paper 4824, May, 1966, pp. 25-58.
27. Serff, N., et al., "Earthquake Induced Deformations of Earth Dams," *Report No. EERC 76-4*, Earthquake Engineering Research Center, University of California, Berkeley, Calif., Sept., 1976.
28. Terzaghi, K., "Mechanisms of Landslides," *The Geological Society of America, Engineering Geology (Berkeley) Volume*, Nov., 1950.
29. Thiers, G. R., and Seed, H. B., "Strength and Stress-Strain Characteristics of Clays Subjected to Seismic Loads," *ASTM STP 450*, Symposium on Vibration Effects of Earthquakes on Soils and Foundations, American Society for Testing and Materials, 1969, pp. 3-56.